

ESTIMATING SEISMIC DEMAND USING SENSOR DATA: EVALUATION OF ELASTIC SPECTRA IN THE LINEAR RANGE OF RESPONSE

Jonathan MONICAL*¹, Benjamin BRITO*², Hamood ALWASHALI*³, Masaki MAEDA*⁴

ABSTRACT

Structural health monitoring (SHM) systems can perform rapid evaluations of buildings damaged in earthquakes by providing reliable measurements of structural properties and seismic demands. This paper summarizes the output of an SHM system used in earthquake simulation tests of small-scale one-story frame specimens focusing on response spectra and the influence of initial period on estimating seismic demand. The data suggest that calculating linear response using elastic spectra and measured periods reduces error by 350% compared with response calculated using estimated periods.

Keywords: structural health monitoring, sensor, seismic demand, linear response, elastic spectra

1. INTRODUCTION

It is costly to hire experienced engineers to make detailed reports of damage for reinforced concrete buildings in the aftermath of major earthquakes. Therefore, rapid damage assessments are preferable to visual observation surveys which take days or weeks to complete. Such assessments may be automated using structural health monitoring (SHM) systems designed for predicting damage. Before investigating the ability of SHM systems to evaluate damage, differences between measured and estimated seismic demand in the linear range of response must be quantified to justify the use of earthquake response spectra in the simplest cases.

Elastic spectra have been used to estimate the response of buildings to earthquakes for decades [1, 2]. For a given strong ground motion, structural response is a function of damping factor and initial period. Damping factors vary with the material of the structure and may be selected using engineering judgement. Fundamental periods of buildings are typically estimated using simple approximations or detailed analysis models. Nevertheless, these estimates may differ from true values by a large margin. The advantage of the SHM system is, after the structure is built, it is possible to obtain accurate estimates of damping and period from sensors installed in buildings.

The purpose of this investigation is two-fold: 1) to report on the accuracy of estimating dynamic properties of simple structures and 2) to quantify differences between the observed linear response of one-story specimens to simulated earthquakes and the estimated response of single-degree-of-freedom oscillators calculated using elastic spectra. Structural response is estimated considering both estimated and measured periods.

2. EXPERIMENTAL PROGRAM

2.1 Test Specimens

Specimens were built as frames using aluminum plates, steel angles, screws, and nuts (Fig. 1). Three types of frame configurations were tested and details of each are listed in Table 1. Estimates of lateral stiffness are calculated assuming fixed-fixed end conditions. Frames had columns made of 2-mm thick, 30-mm wide aluminum plates designed to bend in their weak direction. Bases and roofs of specimens were made of 10-mm thick aluminum plates with lengths and widths of 450 mm.

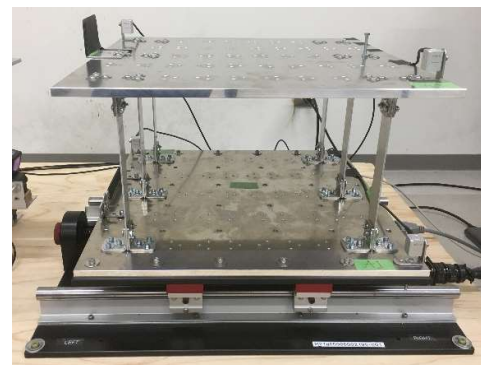


Fig. 1 Elevation of test specimen

Table 1 Frame configurations

Frame	Story height (mm)	Number of columns	Est. lateral stiffness (N/mm)
A1	165	6	21.5
A2	165	4	14.3
A3	215	4	6.5

*1 JSPS Researcher, Department of Architecture and Building Science, Tohoku University, PhD, JCI Member

*2 Researcher, Department of Architecture and Building Science, Tohoku University, PhD

*3 Associate Prof., Graduate School of Environmental and Life Science, Okayama University, PhD, JCI Member

*4 Professor, Department of Architecture and Building Science, Tohoku University, PhD, JCI Member

2.2 Materials

Three aluminum plates were tested in uniaxial tension to measure load-deformation properties of columns used to build specimens. The mean elastic modulus of aluminum was approximately 67,000 MPa (Fig. 2).

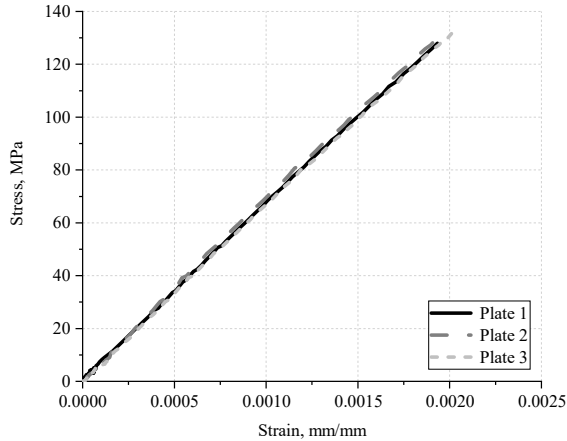


Fig. 2 Aluminum stress-strain curve

2.3 Test Setup

Specimens were clamped to the moving platform of a unidirectional shake table with a maximum rated acceleration of 2.5 g and a full stroke of ± 75 mm. The shake table was bolted to a 100-kg wooden panel to prevent slip during earthquake simulation tests.

2.4 Instrumentation

Displacements at bases and roofs of specimens were measured using two laser displacement sensors attached to an instrumentation frame bolted to the wooden panel (Fig. 3). Displacement sensors had accuracies of approximately 0.02 mm. Two accelerometers were mounted to opposite corners of bases of specimens and two accelerometers were mounted to opposite corners of roofs of specimens. Accelerometers were attached to steel angles clamped to base and roof aluminum plates. Accelerometers had accuracies of approximately 1×10^{-4} g. Measured acceleration data was observed to contain high-frequency noise during earthquake simulations, and a fourth-order Butterworth bandpass filter with a low-pass cut-off frequency of 15 Hz and a high-pass cut-off frequency of 0.25 Hz was used to filter base and roof accelerations.

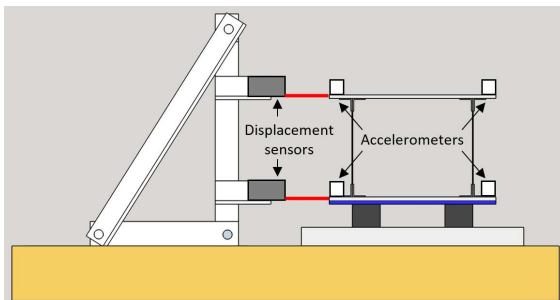


Fig. 3 Instrumentation layout

2.5 Input Ground Motion

The 1940 El Centro record was used as the input base motion for all earthquake simulation tests discussed in this study. The record was downloaded from the Pacific Earthquake Engineering Research (PEER) Center's Ground Motion Database [3]. The "Record Sequence Number" assigned by PEER to the 1940 El Centro record is RSN6. The motion was scaled by a time-compression factor of 2.0 and was reduced in amplitude by a factor of approximately 5.6 to achieve a target PGA of 0.05 g, target PGV of 2.8 cm/sec, and target PGD of 3.9 mm (Fig. 4).

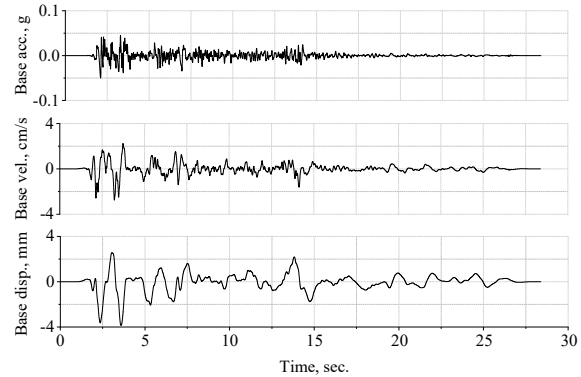


Fig. 4 Input base motion

2.6 Test Sequence

To test a range of periods, steel plates were fastened to roofs of specimens to increase mass while keeping lateral stiffness constant. The effective mass of each specimen was taken as the sum of half of masses of aluminum columns, steel angles, and screws, mass of aluminum plate at roof, and mass of additional steel plates attached to roof. Fundamental initial periods of specimens were between 0.10 and 0.40 seconds (Fig. 5).

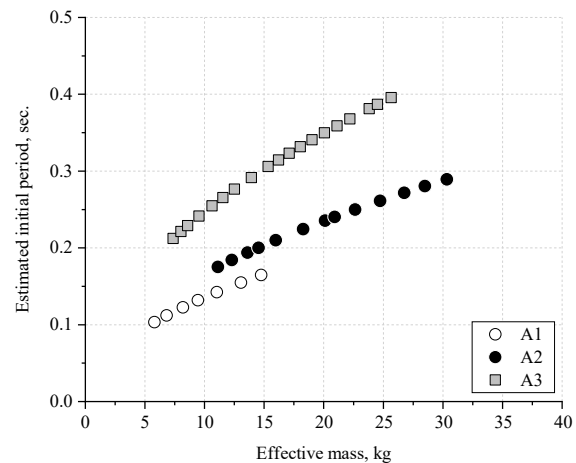


Fig. 5 Estimated initial period vs. effective mass

3. FREE VIBRATION TESTS

Free vibration tests were conducted on specimens prior to earthquake simulation tests to measure lateral stiffnesses, initial periods, and damping factors.

3.1 Lateral Stiffness

Roofs of specimens were pulled with a device measuring load until reaching a story displacement of approximately 1 mm. On average, measurements of lateral stiffness computed as ratios of load to displacement were approximately 5% larger than the estimated values listed in Table 1.

3.2 Initial Period

To observe free vibration response, roofs of specimens were pulled and then released. Initial periods measured during free vibration tests were taken as the inverse of the frequency at peak Fourier response computed as the Fourier decomposition of measured roof acceleration. Initial periods of specimens are estimated using Eq. (1). Periods measured during free vibration tests did not differ from estimated periods by more than 1% on average (Fig. 6).

$$T = 2\pi \times (m/k)^{0.5} \quad (1)$$

where,

T : initial period

m : effective mass

k : lateral stiffness

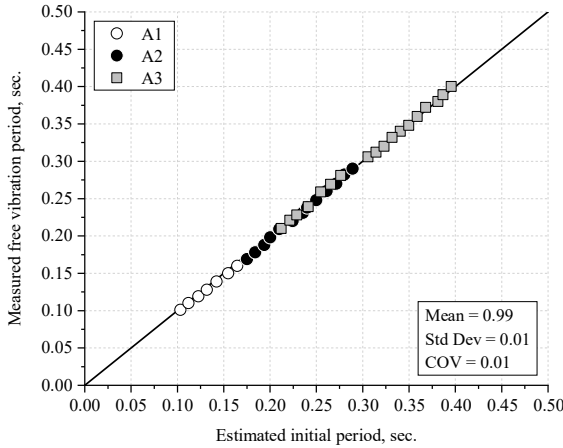


Fig. 6 Period measured during free vibration test vs. estimated initial period

3.3 Damping

Damping observed during free vibration tests is evaluated using Eqs. (2) and (3) assuming structural response decays exponentially with time after initial disturbance [4]. Because the accelerometers used in this investigation have higher resolution than the displacement sensors, acceleration time histories are used for calculation of damping factors. The mean damping factor computed using Eq. (3) was approximately 0.5% for a free vibration test conducted on frame A1 with an initial period of 0.10 seconds (Fig. 7). Free vibration tests conducted on other specimens produced similar responses and a damping factor of 0.5% was selected as the representative damping factor for each specimen.

$$\delta = \ln(a_i / a_{i+1}) \quad (2)$$

$$h = 1 / [1 + (2\pi / \delta)^2]^{0.5} \quad (3)$$

where,

δ : logarithmic decrement

a_i : acceleration at peak i

a_{i+1} : acceleration at peak $i+1$

h : damping factor

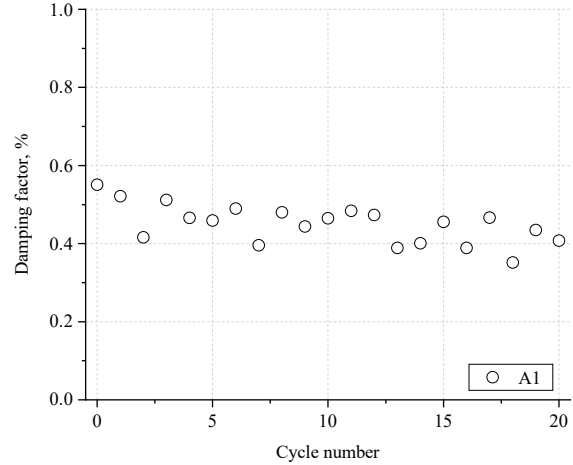


Fig. 7 Damping factor vs. cycle number for frame A1 ($T = 0.10$ sec.)

4. EARTHQUAKE SIMULATION TESTS

Structural response to simulated earthquakes is estimated using elastic spectra and measured base acceleration. Spectra are calculated for a damping factor $h = 0.5\%$ to reflect observed damping factors discussed in Sec 3.3. Spectra are computed using the Newmark-Beta method assuming a gamma factor of 0.5 and a beta factor of 0.25. Spectral values are calculated for periods in increments of 0.001 seconds.

Measurements discussed in this section include spectral acceleration (S_a), spectral displacement (S_d), and initial period (T). Measured S_d is taken as the maximum difference between roof displacement and base displacement obtained from laser displacement sensors. Measured S_a is taken as the maximum absolute roof acceleration obtained from roof accelerometers. Measured initial period is taken as the inverse of the frequency at peak Fourier response computed as the Fourier decomposition of acceleration at roof normalized to the Fourier decomposition of acceleration at base. Results of earthquake simulation tests are discussed next.

4.1 Observed Response

Each specimen ($0.10 \text{ sec.} < T < 0.40 \text{ sec.}$) was subjected to two earthquake simulations, one initial run and one repeat run, to observe the repeatability of the shake table to reproduce base motions. Differences between measurements (S_a , S_d , and T) obtained in initial and repeat runs were no larger than 5% indicating acceptable performance of the shake table.

Measurements of S_a and S_d were observed to coincide closely with estimates of seismic demand computed using measured initial periods and the assumptions stated in Sec. 4 (Figs. 8-9). On average,

measurements of seismic demand were 2-3% larger than estimates of seismic demand with a coefficient of variation (COV) of nearly 7% (Figs. 10-11). These data support the reliability of elastic spectra by demonstrating excellent agreement between observations and estimated response for metallic structures in their linear range.

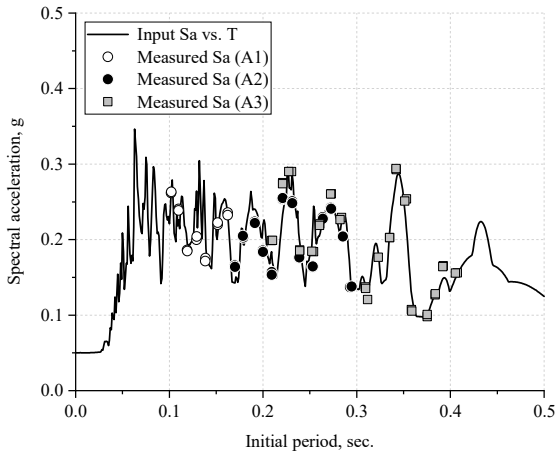


Fig. 8 Comparison of estimated and measured acceleration spectra ($h = 0.5\%$)

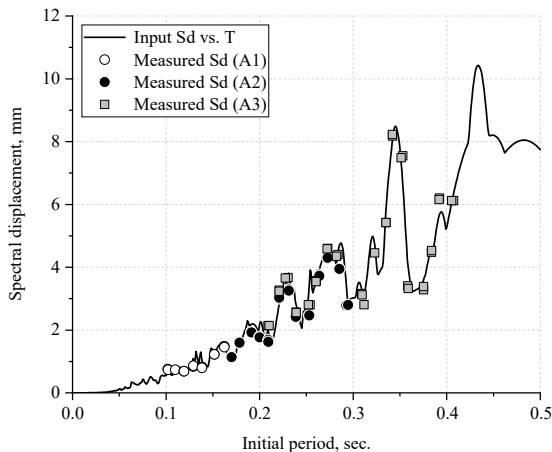


Fig. 9 Comparison of estimated and measured displacement spectra ($h = 0.5\%$)

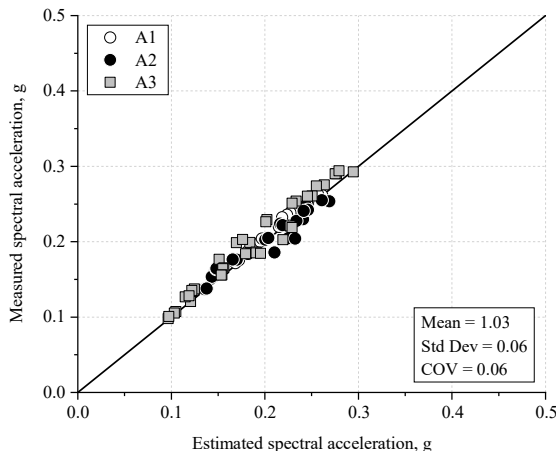


Fig. 10 Measured Sa vs. Estimated Sa computed using measured periods ($h = 0.5\%$)

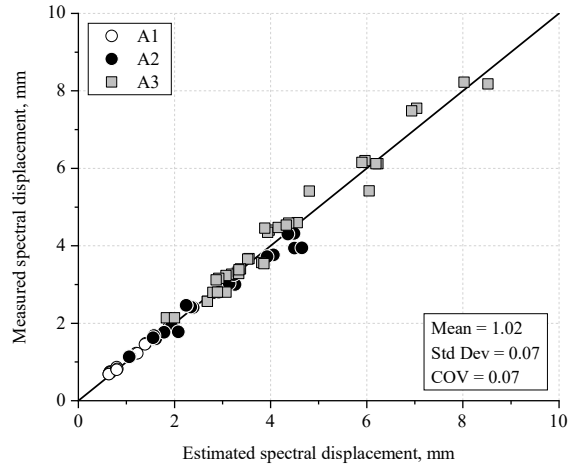


Fig. 11 Measured Sd vs. Estimated Sd computed using measured periods ($h = 0.5\%$)

If no sensor data is available, then measured periods of buildings are unlikely to be known. In such cases, the estimated initial period may be the best representation of the structure. To observe the additional error between observations and spectral response computed using estimated initial periods, measured and estimated spectral displacements are plotted in Fig. 12. Estimates are larger than measurements on average, especially for displacements smaller than 4 mm and for specimens with periods between 0.10 and 0.25 sec.

The overestimation of spectral displacement computed using estimated periods may be related to resonance observed in the short-period range of response spectra concentrated near initial periods of specimens. There are spikes in spectra generated using measured base motion data (compared with spectra generated using input base motion data) at periods slightly longer than measured periods (Fig. 13). Because estimated periods are longer than measured periods on average, estimates of displacement computed using estimated periods are affected by the mentioned spikes and exceed estimates of displacement computed using measured periods (Fig. 14).

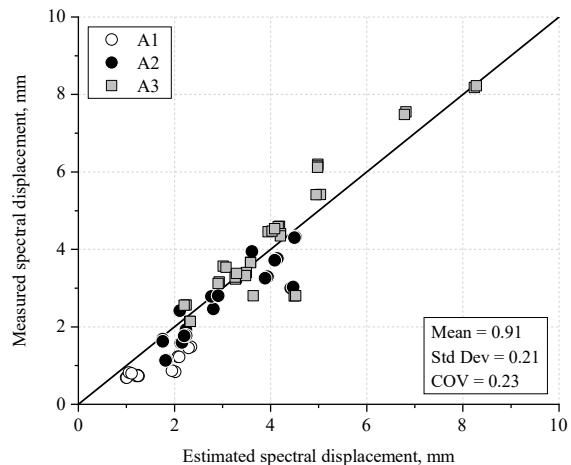


Fig. 12 Measured Sd vs. Estimated Sd computed using estimated periods ($h = 0.5\%$)

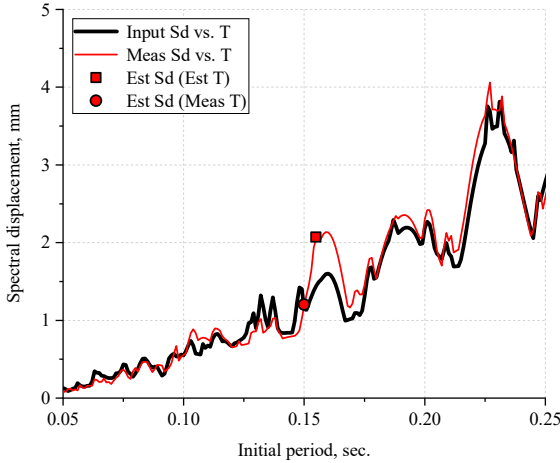


Fig. 13 Input vs. Measured spectra: Estimated Sd computed using estimated periods and measured periods ($T = 0.15$ sec, $h = 0.5\%$)

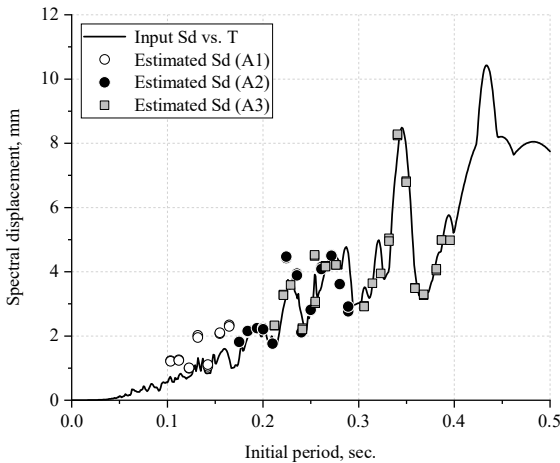


Fig. 14 Estimated Sd computed using spectra generated using measured base motion data and estimated periods

4.2 Smoothing Spectral Shape

One idea for increasing the accuracy of seismic demand calculated using linear spectra and estimated initial periods is to modify spectral shape by “smoothing” regions where small changes in period produce large changes in response. This concept was investigated by projecting the response of a 2% damped system to the response of a 0.5% damped system (Fig. 15). The 2% damped system was uniformly amplified by a factor of approximately 1.3 to produce smoothed response associated with a damping factor of 0.5% (Eqs. 4-5).

The mentioned amplification factor was computed as the mean ratio of spectral response at a given initial period for a 0.5% damped system to that of a 2% damped system averaged over all periods between 0.01-0.50 seconds (Eqs. 6-7). Other smoothing procedures based on amplification factors computed using larger damping factors produced more error than the selected procedure (Fig. 16). Calculating mean amplification factors over smaller ranges of periods increased errors by no more than 2%.

$$Sa_{sm} = F_{Sa} \times Sa_2 \quad (4)$$

$$Sd_{sm} = F_{Sd} \times Sd_2 \quad (5)$$

$$F_{Sa} = \frac{1}{n} \sum_i^n \frac{Sa_{0.5}(Ti)}{Sa_2(Ti)} \text{ for } 0.01s < T < 0.50s \quad (6)$$

$$F_{Sd} = \frac{1}{n} \sum_i^n \frac{Sd_{0.5}(Ti)}{Sd_2(Ti)} \text{ for } 0.01s < T < 0.50s \quad (7)$$

where,

Sa_{sm} : smoothed spectral acc. ($h = 0.5\%$)

Sd_{sm} : smoothed spectral disp. ($h = 0.5\%$)

F_{Sa} : spectral acc. amplification factor

F_{Sd} : spectral disp. amplification factor

$Sa_{0.5}$: spectral acceleration ($h = 0.5\%$)

$Sd_{0.5}$: spectral displacement ($h = 0.5\%$)

Sa_2 : spectral acceleration ($h = 2.0\%$)

Sd_2 : spectral displacement ($h = 2.0\%$)

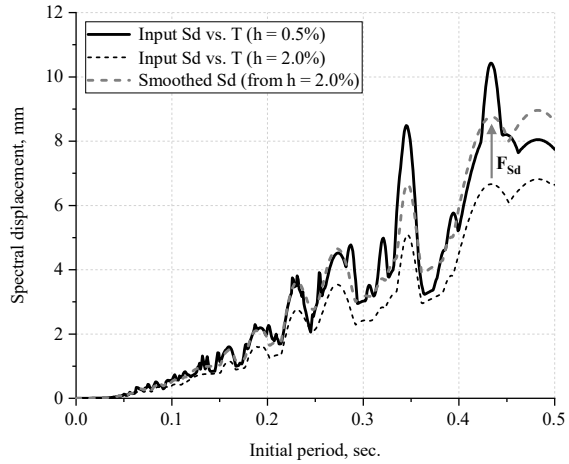


Fig. 15 Procedure for smoothing spectral shape by amplifying 2% damped system

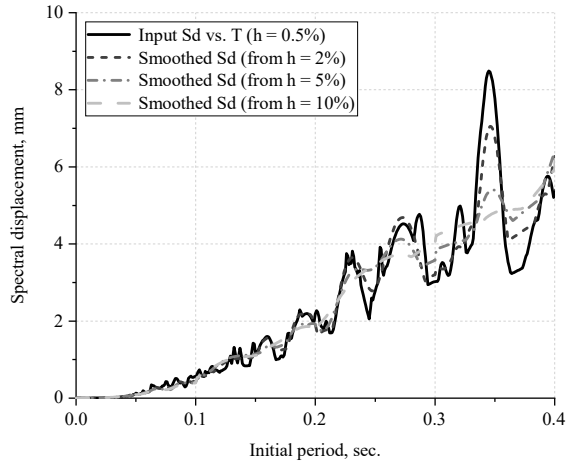


Fig. 16 Projections of 2%, 5%, and 10% damped systems to a 0.5% damped system

To observe the effect of smoothing spectral shape on error when estimating seismic demand in the case where measured periods are unknown, measured and estimated spectral displacements computed using estimated periods are plotted in Fig. 17. The error using smoothed spectra and estimated periods decreased by approximately 30% (based on COV) compared with using unsmoothed spectra. The smoothing procedure

effectively reduced the spikes described in Sec. 4.1 (Figs. 13-14) and produced smaller estimates of displacement in the short-period range (Fig. 18). The advantage of the proposed smoothing procedure is that will likely decrease error in the short-period range of response because of the issues with resonance observed in response spectra.

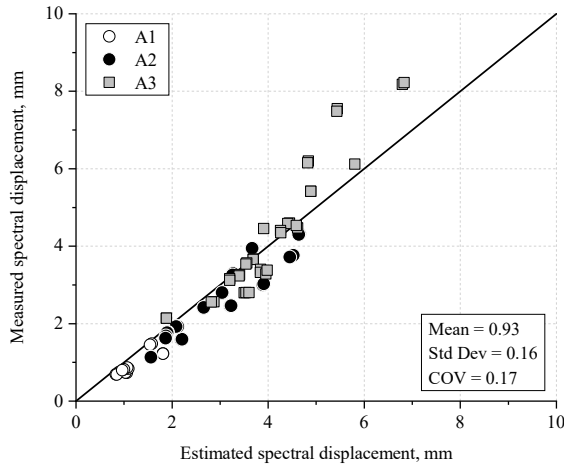


Fig. 17 Measured Sd vs. Estimated Sd computed using smoothed spectra and estimated periods

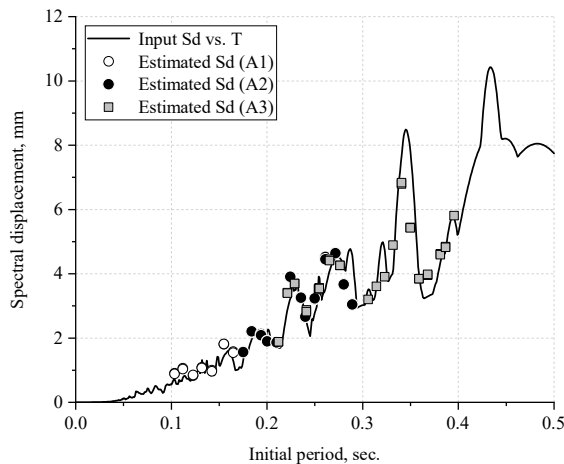


Fig. 18 Estimated Sd computed using smoothed spectra generated using measured base motion data and estimated periods

5. SUMMARY

The results described in Sec. 3 and Sec. 4 highlight the advantages of using sensor data to estimate seismic demands. Although estimates of periods are only 1% longer than measured periods on average, calculating seismic demand using estimated periods produces large errors. This tendency emphasizes the need for SHM systems even for simple structures and supports the reliability of linear response when computed using 1) measured initial periods of structures and 2) damping factors inferred from free vibration response.

6. FUTURE WORK

The next phase of this project consists of 1) conducting earthquake simulation tests on multiple-degree-of-freedom (MDOF) aluminum frame structures in the linear and nonlinear range of response, and 2) investigating the influence of measured periods on estimating structural response of reinforced concrete structures. Based on the results of 1) and 2), procedures similar to those discussed in this study will be recommended for accurately estimating seismic demand and identifying when structures become severely damaged.

7. CONCLUSIONS

- (1) Damping factors measured during exponentially decreasing response observed during free vibration tests represent reasonable estimates of viscous damping used to generate elastic spectra.
- (2) Estimating seismic demand using measured initial periods produces an error 3.5 times smaller than the error produced by estimating seismic demand using estimated initial periods.
- (3) In cases where no measured periods are available, calculating seismic demand using estimated periods and smoothed response spectra decreases error by approximately 30% compared with computations based on unsmoothed spectra.

ACKNOWLEDGEMENTS

This work was supported by JAEA Nuclear Energy S&T and Human Resource Development Project “建屋応答モニタリングと損傷イメージング技術を活用したハイブリッド型の原子炉建屋長期健全性評価法の開発研究” (Grant Number JPJA21P12345678, Principal researcher: Prof. Masaki MAEDA, Tohoku University). The authors would like to thank Dr. Matsutaro SEKI for his comments on this manuscript.

REFERENCES

- [1] Housner, G. W. (1952). “Spectrum Intensities of Strong-Motion Earthquakes,” Proceedings of the Symposium on Earthquake and Blast Effects on Structures, Los Angeles, California. Earthquake Engineering Research Institute, pp. 20-36.
- [2] Newmark, N. M. (1959). “A Method of Computation for Structural Dynamics,” Journal of the Engineering Mechanics Division, Vol. 85, No. EM3, pp. 67-94.
- [3] Ancheta, T., et. al (2014). “NGA-West2 Database”. Earthquake Spectra, Vol. 30, No. 3, pp. 989-1005.
- [4] Biggs, J. M. (1964). “Introduction to Structural Dynamics,” McGraw-Hill, Chapter 2: Rigorous Analysis of One-degree Systems, pp. 51-54.